OH-LIF measurement of $H_2/O_2/N_2$ flames in a micro flow reactor with a controlled temperature profile

T Shimizu[1], **H Nakamura**[1], **T Tezuka**[1], **S Hasegawa**[1] **and K Maruta**[1,2].

[1]Institute of Fluid Science, Tohoku University, 2-1-1, Aoba-ku, Sendai, Miyagi, 980-8577, Japan

[2]Far Eastern Federal University, 8 Suhanova St., Vladivostokok 690950, Russia

E-mail: shimizu@edyn.ifs.tohoku.ac.jp

Abstract. This paper presents combustion and ignition characteristic of $H_2/O_2/N_2$ flames in a micro flow reactor with a controlled temperature profile. OH-LIF measurement was conducted to capture flame images. Flame responses were investigated for variable inlet flow velocity, U, and equivalence ratio, ϕ. Three kinds of flame responses were experimentally observed for the inlet flow velocities: stable flat flames (normal flames) in the high inlet flow velocity regime; unstable flames called *Flames with Repetitive Extinction and Ignition* (FREI) in the intermediate flow velocity regime; and stable weak flames in the low flow velocity regime, at ϕ = 0.6, 1.0 and 1.2. On the other hand, weak flame was not observed at ϕ = 3.0 by OH-LIF measurement. Computational OH mole fractions showed lower level at the rich conditions than those at stoichiometric and lean conditions. To examine this response of OH signal to equivalence ratio, rate of production analysis was conducted and four kinds of major contributed reaction for OH production: R3($O + H_2 <=> H + OH$); R38($H + O_2 <=> O + OH$); R46($H + HO_2 <=> 2OH$); and R86($2OH <=> O + H_2O$), were found. Three reactions among them, R3, R38 and R46, did not showed significant difference in rate of OH production for different equivalence ratios. On the other hand, rate of OH production from R86 at ϕ = 3.0 was extremely lower than those at ϕ = 0.6 and 1.0. Therefore, R86 was considered to be a key reaction for the reduction of the OH production at ϕ = 3.0.

1. Introduction

Hydrogen produced by renewable energies attracts attentions as one of the alternative fuels for petroleum fuels. Hydrogen has huge energy per unit mass and its combustion never exhausts carbon dioxide because it contains no carbon atom. However, it is important to investigate combustion characteristics to develop practical combustion devices because the present knowledge on hydrogen combustion is not sufficient.

This study employed a micro flow reactor with a controlled temperature profile (MFR)[1] to investigate hydrogen combustion. This reactor has a narrow channel, whose diameter is smaller than the ordinary quenching diameter, and the channel is heated by an external heat source to give a stationary temperature profile along the inner surface of the reactor. This reactor has been applied for various hydrocarbons in our past studies [1, 2]. They showed three kinds of flame responses for variable inlet flow velocities: stable flat flames (normal flames) in the high inlet flow velocity regime; unstable flames called *Flames with Repetitive Extinction and Ignition* (FREI) in the intermediate flow velocity regime; and stable weak flames in the low flow velocity regime. Especially, weak flames were often studied because the weak flame branch was regarded as a part of the ignition branch of

Fendell curve [3] in the theoretical analysis [4] and unsteady multi-stage oxidation of hydrocarbons was examined by stable multiple weak flames [2].

In our previous study for $H_2/O_2/N_2$ mixture using a MFR, two kinds of flame responses were experimentally observed for variable inlet flow velocities, U, by measurements of OH chemiluminescence using an UV camera [5]. One is normal flame in U > 70 cm/s and another is FREI in U = 11 - 70 cm/s. Gas sampling and analysis showed the consumption of H_2 and 1-D computational results indicated the existence of weak flame. However, weak flame was not observed in the low inlet flow velocity regime experimentally. Mantzaras et al. conducted 3-D numerical simulation of hydrogen flames in a heated micro channel [6-8] and they showed axisymmetric combustion modes for U = 0.5 – 500 cm/s in tube diameter of d = 1.0 mm [8]. Steady mild combustion in the low flow velocity, oscillatory ignition / extinction in the intermediate flow velocity and steady flames in the high flow velocity were obtained at ϕ = 0.5.

Thus, the existence of weak flame of $H_2/O_2/N_2$ mixture is still an open question. Therefore, the existence of weak flame of $H_2/O_2/N_2$ mixture was investigated by OH-LIF measurement at various ϕ (0.6, 1.0, 1.2 and 3.0) in this study.

2. Experiment and computation

2.1. Experimental setup and conditions

A schematic of experimental setup is shown in Figure 1. A quartz tube with an inner diameter of 2 mm was used as a reactor channel and was heated by a H_2/air flat-flame burner to obtain a stationary temperature profile from 300 K to 1300 K along the inner surface of the reactor. A $H_2/O_2/N_2$ mixture was supplied to the reactor. The mixture was diluted in $H_2/O_2/N_2$ = 2:1:9. Flame responses to variable inlet flow velocity were observed by OH-LIF measurement. Wavelength of 283 nm by DYE-Laser (FINE ADJUSTMENT, 0312P043) which was converted from 532 nm of Nd:YAG-Laser (LOTIS TII, LS-2137/3) was chosen to excite OH. A laser beam was run through a pinhole with diameter of 2 mm after concentrated by convex and concave lens. The laser was introduced from the downstream side of the reactor. An image-intensified CCD camera (ANDOR, DH334T-18-E3) with UV lens, an OH band-pass filter (center wavelength: 313 nm; half value width: 10 nm; and transmissivity > 60%) and two 300 nm high-pass filters were used to capture flame images. Background subtraction image processing was done for captured images. All experiments were conducted at atmospheric pressure.

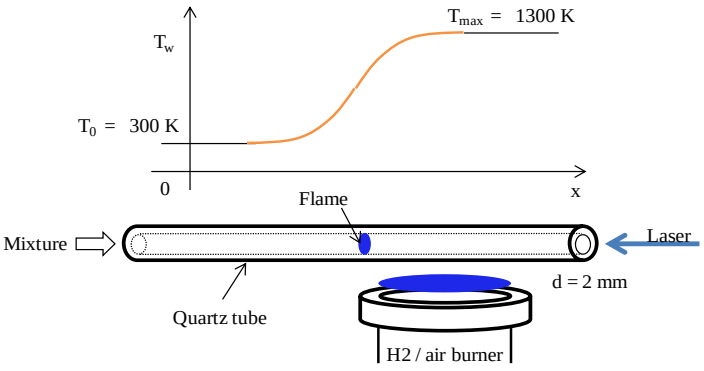

Figure 1. Schematic of experimental setup and provided wall-temperature profile.

2.2. Definition of flame locations

The peak position in the luminosity profile of OH-LIF images was selected to define the normal flame position because 1-D computation showed that the peak position in the heat release rate (HRR) profile

corresponded to that in the OH mole fraction profile. On the other hand, the position of the half maximum in OH profile rise was used for that of weak flame because it agrees with the position of the HRR peak for weak flames in the computation. For FREIs, wall temperatures at the extinction and ignition positions were identified from the upstream and downstream edge of more than 50 instantaneous OH-LIF images.

2.3. Computational conditions

One-dimensional steady-state flame code based on PREMIX was used [1]. The energy equation includes convective heat transfer between gas and wall. Four kinds of mechanism (GRI 3.0 [9], San Diego Mech. [10], Princeton H_2-O_2 Model [11] and Aramco Mech. 1.3 [12].) were used to examine their performances in the present reactor. Computations were conducted for the same conditions as those of the present experiments.

3. Results and discussions

3.1. Flame responses to equivalence ratio and inlet flow velocity

Figure 2 shows observed flame responses to the inlet flow velocity at $\phi = 1.0$. Three kinds of flame responses to the inlet flow velocity were observed: normal flame in the high flow velocity regime; FREI in the intermediate flow velocity regime; and weak flame in the low flow velocity regime. These three kinds of flame responses were observed not only at $\phi = 1.0$ but also at $\phi = 0.6$ and 1.2. At $\phi = 3.0$, however, weak flames were not observed while normal flames and FREI were observed.

The measured flame positions were shown in Figure 3. Normal flames shift to the lower temperature side with the decrease of the inlet flow velocity for all equivalence ratios studied. Normal flames at $\phi = 1.2$ and 3.0 are located at the lower temperature region than those at $\phi = 0.6$ and 1.0. Weak flames shift to the higher temperature side with the decrease of the inlet flow velocity. Weak flames at $\phi = 1.2$ are located at the lower temperature region than those at $\phi = 0.6$ and 1.0.

Figure 4 shows computational HRR peak positions at various inlet flow velocities and equivalence ratios. Normal flames shift to the lower temperature side with the decrease of the inlet flow velocity for all equivalence ratio studied and normal flames at $\phi = 1.2$ and 3.0 are located at the lower temperature region than those at $\phi = 0.6$ and 1.0 which are the same tendencies in the experiment. Steady solutions were not obtained in the intermediate flow velocity region where unsteady solutions of FREI were expected. Weak flames were not observed in the experiment at $\phi = 3.0$ but weak flame solutions in the low flow velocity region were obtained in the computation.

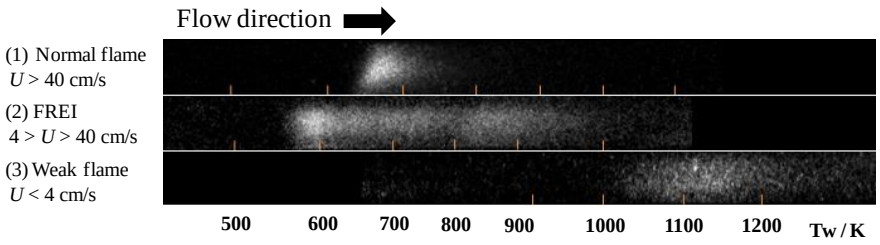

Figure 2. Flame responses captured by OH-LIF measurements at ϕ=1.0.

3.2. OH concentration for variable equivalence ratios

A reason why OH-LIF was not able to obtain weak flames at $\phi = 3.0$ was investigated by computations. Figure 5 shows that the maximum OH mole fractions for variable equivalence ratios. The maximum OH mole fraction was extremely decreased in the rich side. This low level of OH mole fraction made the OH-LIF measurement difficult to observe weak flames at $\phi = 3.0$. Rate of production analysis was conducted for OH to investigate the significant decrease of OH mole fraction in the rich side. GRI 3.0 was used for this analysis because the computational weak flame position with GRI 3.0 was in the best agreement with the experimental flame position compared with the other mechanisms.

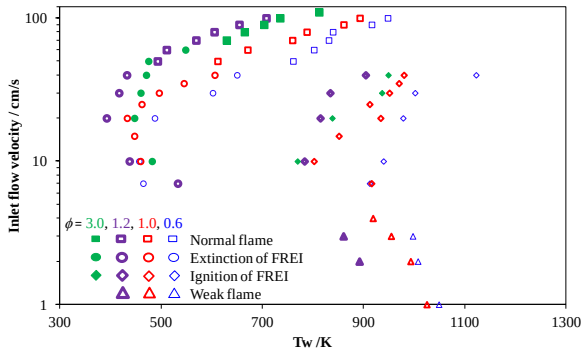

Figure 3. Measured flame position and extinction and ignition points of FREI in various flow velocities at $\phi = 0.6$, 1.0, 1.2 and 3.0.

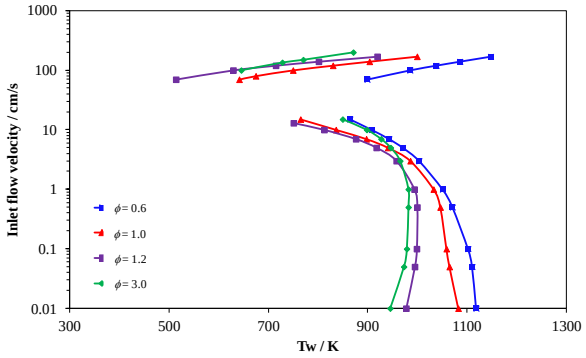

Figure 4. Computational HRR peak positions in various flow velocities at $\phi = 0.6$, 1.0, 1.2 and 3.0.

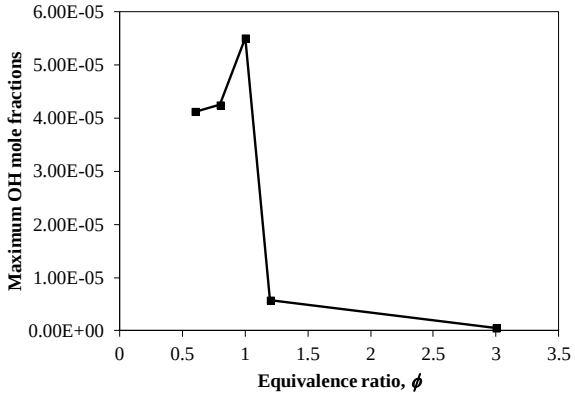

Figure 5. Maximum OH mole fraction for variable equivalence ratios in computation.

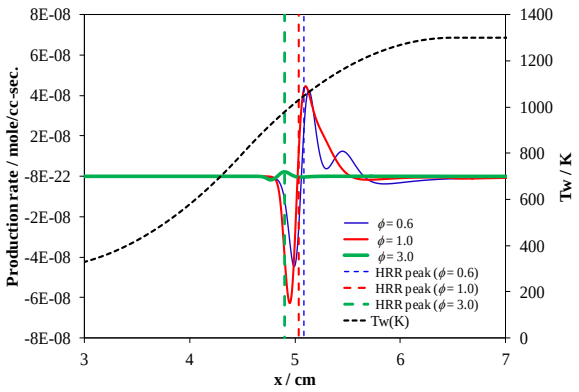

Figure 6. Computational net rate of OH production at $\phi = 0.6$, 1.0 and 3.0.

Net rate of OH production at $\phi = 0.6$, 1.0 and 3.0 were shown in Figure 6. Net rate of OH production at $\phi = 3.0$ was much lower than those at $\phi = 0.6$ and 1.0. Major contributed reactions for OH production were investigated at the HRR peak position. As a result, four major contributed reactions for OH production were found: R3($O + H_2 <=> H + OH$); R38($H + O_2 <=> O + OH$); R46($H + HO_2 <=> 2OH$); and R86($2OH <=> O + H_2O$). Three of them, R3, R38 and R46, did not show big difference between $\phi = 3.0$ and $\phi = 0.6$ and 1.0. However, R86, which forms OH radicals through the backward reaction, became significantly small at $\phi = 3.0$. Therefore, it is considered that the low level of OH mole fraction in the rich side would be due to the equivalence ratio dependence of R86.

4. Conclusion

Ignition and combustion characteristics of $H_2/O_2/N_2$ flames were investigated using a micro flow reactor with a controlled temperature profile at various equivalence ratios and inlet flow velocities. OH-LIF measurement was applied for capturing flame images. As a result, three kinds of flame responses: normal flame in the high inlet flow velocity regime; FREI in intermediate flow velocity regime; and weak flame in the low flow velocity regime, were experimentally observed at ϕ = 0.6, 1.0 and 1.2. On the other hand, only two kinds of flame responses: normal flame and FREI, were observed at ϕ = 3.0. Computational OH mole fraction was remarkably decreased in the rich conditions. Therefore it is considered that weak flames were not observed in experiment at ϕ = 3.0. Rate of production analysis was conducted to find the difference in reaction process at ϕ = 0.6, 1.0 and 3.0. Four major reactions for OH production: R3($O + H_2 <=> H + OH$); R38($H + O_2 <=> O + OH$); R46($H + HO_2 <=> 2OH$); and R86($2OH <=> O + H_2O$), were identified. The reaction rates of R3, R38, R46 were not changed so much when the equivalence ratio was varied but the reaction rate of R86 became significantly small at ϕ = 3.0.

Acknowledgement

The part of the study was supported financially by the Ministry of education and science of Russian Federation (project 14. Y26.31.0003).

References

[1] Maruta K, Kataoka T, Kim I. N, Minaev S. and Fursenko R, 2005 *Proc. Combust. Inst.* **30** 2429-2436.

[2] Yamamoto A, Oshibe H, Nakamura H, Tezuka T, Hasegawa S. and Maruta K, 2011 *Proc. Combust. Inst.* 2 **33** 3259-3266.

[3] Nakamura H, Yamamoto A, Hori M, Tezuka T, Hasegawa S and Maruta K, 2013 *Proc. Combust. Inst.* **34** 3435-3443.

[4] Minaev S, Maruta K and Fursenko R, 2007 *Combust. Theor. Model* 2 **11** 187-203.

[5] Saruwatari K, Nakamura H, Tezuka T, Hasegawa S and Maruta K, 2012 *ICFD* OS11.

[6] Pizza G, Frouzakis E. C, Mantzaras J, Tomboulides A. and Boulouchos K. 2008 *Comb. Flame* **152** 433-450.

[7] Pizza G, Frouzakis E. C, Mantzaras J, Tomboulides A. and Boulouchos K. 2008 *Comb. Flame* **155** 2-20.

[8] Pizza G, Frouzakis E. C, Mantzaras J, Tomboulides A. and Boulouchos K. 2010 *J. Fluid Mech.* **658** 463-491.

[9] Smith G. P, Golden D. M, Frenklach M, Moriarty N. W, Eiteneer B, Goldenberg M, Bowman C. T, Hanson R. K, Song S, Gardiner W. C. Jr. Lissianski V. V, Qin Z. GRI-Mech 3.0. Available at http://www.me.berkeley.edu/gri mech/.

[10] Prince J. C, Williams F. A, 2011 *Proc. 7th U. S. National Tech. Meeting Combust. Inst*, 20-23 Available at http://web.eng.ucsd.edu/mae/groups/combustion/mechanism.html.

[11] Burke M. P, Chaos M, Ju Y, Dryer F. L and Klippenstein S. J, 2004 *Int. J. Chem. Kinet*. **36** 566-575 Available at http://www.princeton.edu/mae/people/faculty/dryer/homepage/kinetic_models/h2-o2-model-update/.

[12] Metcalfe W. K, Burke S. M, Ahmed S. S, Curran H. J, 2013 *Int. J. Chem. Kinet.* 10 **45** 638–675 Available at http://www.nuigalway.ie/c3/Mechanism_release/frontmatter.html.